Plant, Cell and Environment (2004) **27**, 641–653

Sites of actin filament initiation and reorganization in cold-treated tobacco cells

J. POKORNÁ[1], K. SCHWARZEROVÁ[1], S. ZELENKOVÁ[1], J. PETRÁŠEK[1,2], I. JANOTOVÁ[1,2], V. ČAPKOVÁ[1,2] & Z. OPATRNÝ[1]

[1]*Department of Plant Physiology, Charles University, Faculty of Science, Viničná 5, 128 44 Prague 2, Czech Republic and* [2]*Institute of Experimental Botany, Academy of Sciences of the Czech Republic, Prague, Czech Republic*

ABSTRACT

Cytoskeletal proteins assemble into dynamic polymers that play many roles in nuclear and cell division, signal transduction, and determination of cell shape and polarity. The distribution and dynamics of microtubules (MTs) and actin filaments (AFs) are determined, among other factors, by the location of their nucleation sites. Whereas the sites of microtubule nucleation in plants are known to be located under the plasma membrane and on the nuclear envelope during interphase, there is a striking lack of information about nucleation sites of AFs. In the studies reported herein, low temperature (0 °C) was used to de-polymerize AFs and MTs in tobacco BY-2 (*Nicotiana tabacum* L.) cells at interphase. The extent of de-polymerization of cytoskeletal filaments in interphase cells during cold treatment and the subcellular distribution of nucleation sites during subsequent recovery at 25 °C were monitored by means of fluorescence microscopy. The results show that AFs re-polymerized rapidly from sites located in the cortical region and on the nuclear envelope, similarly to the initiation sites of MTs. In contrast to MTs, however, complete reconstitution of AFs was preceded by the formation of transient actin structures including actin dots, rods, and filaments with a dotted signal. Immunoblotting of soluble and sedimentable protein fractions showed no changes in the relative amounts of free and membrane-bound actin or tubulin.

Key-words: *Nicotiana tabacum*; actin; actin filaments; cold stress; cytoskeleton; microtubules; tobacco cells BY-2; tubulin.

INTRODUCTION

The cytoskeleton is a highly dynamic structure that plays many roles in nuclear and cell division, signalling, determination of cell shape and polarity, and cell motility. Two main components of the cytoskeleton, tubulin polymerizing into microtubules (MTs) and actin polymerizing into actin filaments (AFs), are found in all eukaryotic cells. Protein complexes that assist in the nucleation of polymers appear to be composed of evolutionarily highly conserved proteins. For microtubule nucleating sites, γ-tubulin has been identified as a universal nucleator (Wiese & Zheng 1999). It functions in a protein complex belonging to the Spc97p/Spc98p protein family originally identified in fungi (Knop & Schiebel 1997). Their homologues have been identified in animals (Murphy, Urbani & Stearns 1998) as well as in plants (Erhardt *et al*. 2002). Despite the conserved nature of cytoskeletal proteins, however, MT arrays differ substantially among various organisms and cell types. Plant cells lack centrosomes, which nucleate interphase MTs and organize mitotic spindles in animal cells. Instead, plant MTs are nucleated in a cell cycle-dependent manner from multiple nucleation sites localized on the nuclear surface and in the cortical cytoplasm (Hasezawa, Kumagai & Nagata 1997).

In contrast to microtubule initiation, eukaryotic cells possess multiple mechanisms of initiation of actin assembly. These include *de novo* actin nucleation, uncapping of barbed ends, and severing of existing filaments (Condeelis 2001). In animal, fungal and protozoan cells, *de novo* actin polymerization driven by the actin-related protein 2/3 (Arp2/3) complex is a well-understood mechanism (Machesky & Gould 1999). Much less information is available on actin nucleating sites in plant cells. An Arp2/3 protein complex consists of seven subunits and conserved DNA coding sequences for all of them are present in the *Arabidopsis* genome (Vantard & Blanchoin 2002). Mutations in *Arabidopsis* Arp2 and Arp3 genes result in actin rearrangement in some cells, accompanied by malformations of cell shape (Mathur *et al*. 2003). Thus, it seems that Arp 2/3-based actin polymerization represents a conserved mechanism, although detailed information about the molecular composition, subcellular localization, and regulation of the Arp 2/3 complex in plants remains enigmatic.

AFs have been shown to form the backbones of cytoplasmic strands in vacuolated plant cells (Esseling, de Ruijter & Emons 2000). They form a dense network that co-aligns with microtubules in the cortical cytoplasm, wind around the nucleus forming a basket, and are localized to the

Correspondence: Kateřina Schwarzerová. E-mail: schwarze@natur.cuni.cz

mitotic spindle and the phragmoplast (Kakimoto & Shibaoka 1987). Furthermore, actin-based molecular motors drive the motility of tubular endoplasmic reticulum (Liebe & Menzel 1995), Golgi vesicles (Nebenführ *et al*. 1999), plastids (Takagi 2000), and mitochondria (Van Gestel, Kohler & Verbelen 2002). Although the organization of actin cytoskeleton and the role of various actin arrays in plant cells seem to be well known, the sites of actin initiation, reorganization, and their subcellular distribution have not been described.

To study the processes of cytoskeleton dynamics in plant cells, various stress factors can be used to induce the destruction and subsequent recovery of the cytoskeleton. Among other agents, low temperature is known to de-polymerize cytoskeletal polymers. The structure of MT arrays in cells subjected to cold treatment has been studied thoroughly, and cold-induced de-polymerization of MTs has been documented to vary in a wide range of plant species (for review see Nick 2000). Experiments with cold-treated tobacco BY-2 cells showed that MTs in actively dividing cells in the exponential phase of growth were more sensitive to cold than those in non-dividing cells in the stationary phase of growth (Mizuno 1992). A subset of MTs in tobacco BY-2 cells in the stationary phase of growth were shown to be cold-stable (Akashi, Kawasaki & Shibaoka 1990) and their complete de-polymerization was achieved only by a combination of cold and application of anti-microtubular drugs (Hasezawa *et al*. 1997). These authors took advantage of the reversible de-polymerization of MTs after removal of the drug and cultivation of the cells at 30 °C, and observed sites of nucleation of new MTs. Much less information is available concerning low temperature-induced changes in the actin cytoskeleton. The role of AFs was studied in relation to cold-induced cessation of cytoplasmic streaming (Quader, Hofmann & Schnepf 1989) and changes in membrane fluidity (Örvar *et al*. 2000), but information about the effects of cold on the organization of AFs and the sites of their initiation is sparse (Egierszdorff & Kacperska 2001).

The goal of this study was to determine the pattern of AF de-polymerization in tobacco BY-2 cells exposed to 0 °C, and then follow the sites of AF initiation and the pattern of their re-assembly during recovery at 25 °C. In addition, de-polymerization and assembly of MTs were also monitored in order to compare the sites of initiation and reorganization of both cytoskeletal components. Here we show that after cold-induced de-polymerization, AFs re-polymerized quickly from nucleation sites that were located in the cortical cytoplasm and on the nuclear envelope, similarly to the initiation sites of MTs. In contrast to MTs, however, complete reconstitution of AFs was preceded by the formation of transient actin structures including actin dots, rods, and filaments with a dotted signal, and newly formed actin filaments were always branched. Immunoblotting of soluble and sedimentable protein fractions revealed no changes in the relative amounts of free and membrane-bound actin or tubulin.

MATERIALS AND METHODS

Plant material and chemicals

The tobacco cell line BY-2 (*Nicotiana tabacum* L. cv. Bright Yellow 2; Nagata, Nemoto & Hasezawa 1992) was cultured in liquid medium containing 4.3 g L^{-1} MS salts (Sigma, St Louis, MO, USA), 1 mg L^{-1} thiamine, 200 mg L^{-1} KH_2PO_4, 100 mg L^{-1} inositol, 30 g L^{-1} sucrose and 0.2 mg L^{-1} (0.9 μM) 2,4-dichlorophenoxyacetic acid (2,4-D), pH 5.8. Every 7 d, 1.5 mL of cells were transferred to 30 mL of fresh medium and cultured in darkness at 25 °C on a horizontal shaker (IKA KS501; IKA Labortechnik, Staufen, Germany; 120 r.p.m., orbital diameter 30 mm). All chemicals were obtained from Sigma unless otherwise stated.

Cold treatment and recovery experiments

Tobacco BY-2 cells in the exponential phase of growth (3-day-old) were used for all experiments. A standard cell population in this phase of growth consists of 85–95% cells in interphase and 5–15% cells in mitosis and cytokinesis. In all cytological observations, only interphase cells were analysed. Cultivation conditions and cold treatments were carefully optimized to exclude any additional stress. Cell suspensions in Erlenmayer flasks were placed in an ice water bath (0 °C) and shaken on a horizontal shaker at 100 r.p.m. (IKA KS501; IKA Labortechnik) in darkness. For recovery experiments, flasks were removed from the ice water bath after 12 h of cold treatment and the cells were immediately collected by filtering on a nylon mesh (pore diameter 20 μm). The cells were then re-suspended in a medium at the control temperature (25 °C) and further cultivated at 25 °C. During the periods of cold treatment and subsequent recovery at control temperature, samples of cell culture were collected for cytological observations and protein extraction.

Determination of cell viability

Cell viability was assessed with fluorescein diacetate (FDA) according to the method of Widholm (1972). Forty microlitres of 0.2% (w/v) FDA stock solution in acetone were diluted with 7 mL of culture medium, and an aliquot mixed 1 : 1 (v/v) with cell suspension on a microscopic slide. After a 1-min incubation with FDA, the viability was determined from at least 10 optical fields on each of five separate slides as a percentage of fluorescing cells (a total of about 400 cells were counted in each sample). Prior to the measurement of viability of the cold-treated cells, aliquots of cell culture were taken, filtered, re-suspended in the same volume of cultivation medium at 25 °C, and cultivated on a horizontal shaker (IKA KS501; IKA Labortechnik) at 120 r.p.m and 25 °C for 2 h.

Visualization of actin filaments

AFs were visualized by the method of Kakimoto & Shibaoka (1987) modified according to Olyslaegers & Verbelen

(1998). A 1-mL volume of 3-day-old cell culture was fixed for 10 min in 1.8% (w/v) paraformaldehyde (PFA) in standard buffer [50 mM piperazine-1,4-bis(2-ethanesulfonic acid) (PIPES), pH 7, supplemented with 5 mM $MgCl_2$, and 10 mM ethylenebis(oxyethylenenitrilo)tetraacetic acid (EGTA)]. Cold-treated cells were prefixed for 5 min in fixation solution chilled to 0 °C. After a subsequent 10-min fixation in standard buffer containing 1% glycerol, cells were rinsed twice for 10 min with standard buffer. Then 0.5 mL of the re-suspended cells were incubated for 35 min in an Eppendorf tube with the same amount of 0.66 μM tetramethylrhodamine isothiocyanate (TRITC) – phalloidin freshly prepared from a 6.6 μM stock solution in 96% (v/v) ethanol by diluting 1 : 10 with phosphate-buffered saline (PBS; 0.15 M NaCl, 2.7 mM KCl, 1.2 mM KH_2PO_4, 6.5 mM Na_2HPO_4). Cells were then washed three times for 10 min in PBS and observed immediately in the microscope.

Visualization of microtubules

MTs were visualized as described by Wick *et al*. (1981) with the modifications of Mizuno (1992). Briefly, 3 mL of 3-day-old cell culture were fixed for 30 min in 3.7% (w/v) PFA in microtubule stabilizing buffer (MSB) consisting of 50 mM PIPES, 2 mM EGTA, 2 mM $MgSO_4$, pH 6.9, at 25 °C and the cells were subsequently post-fixed for 20 min in 3.7% (w/v) PFA in MSB supplemented with 1% Triton X-100. Cold-treated cells were prefixed for 10 min in fixation solution chilled to 0 °C. After digestion with an enzyme solution [1% (w/v) macerozyme and 0.2% (w/v) pectinase] for 7 min at 25 °C, the cells were attached to poly L-lysine-coated coverslips and extracted with 1% (v/v) Triton X-100 in MSB for 20 min. Subsequently, the cells were treated with 0.5% (w/v) bovine serum albumin (Fluka, Buchs, Switzerland) in PBS for 30 min and incubated with a monoclonal mouse antibody against α-tubulin N356 (Amersham Biosciences, Europe GmbH, Freiburg, Germany) for 45 min at 25 °C (dilution 1 : 500 in PBS). After washing with PBS, a secondary fluorescein isothiocyanate (FITC)-conjugated anti-mouse antibody diluted 1 : 80 in PBS was applied for 1 h at 25 °C. Specimens were washed in PBS, embedded in 50% glycerol supplemented with Hoechst 33258 [bisbenzimide, 2-(4-ethoxyphenyl)-5-(4-methyl-1-piperazinyl); 0.1 μg mL^{-1}] to stain nuclei and observed immediately in the microscope.

Microscopy and image adjustment

For all observations, we used an epifluorescence microscope (Olympus Provis AX 70; Olympus Optical Co., Ltd, Tokyo, Japan) equipped with standard filter sets for detection of FITC, TRITC and Hoechst 33258 fluorescence and Nomarski differential interference contrast (DIC). Fluorescence images were taken using a monochrome integrating CCD camera (COHU 4910; Cohu, Inc., Poway, CA, USA) and DIC images with a 3 CCD color video camera (SONY DXC-950P; Sony Corp., Tokyo, Japan). All images were stored digitally using LUCIA image analysis software (Laboratory Imaging, Prague, Czech Republic).

Quantification of cold-induced changes in the arrangement of actin filaments and microtubules

The percentages of cells with distinct cytoskeleton arrangements were determined from at least 10 optical fields on each at least three separate slides (a total of around 300 cells were counted in each sample) in one representative experiment. For quantification of structural changes in cytoskeleton during cold treatment, the following categories were defined: (1) cells retaining intact cytoskeletal filaments or their fragments; (2) cells with totally de-polymerized cytoskeleton; (3) cells with cold-induced re-organization of cytoskeleton; and (4) damaged cells. The last category included cells with disrupted cytoplasm, broken cell walls, or cells with plasma membrane detached from the cell wall. In controls, the numbers of such cells were approximately 10 and 15% for MTs and AFs, respectively. In cell culture maintained at 0 °C for 12 h, the number of cells with unsatisfactorily visualized cytoskeletons increased to 40–50%. The phase of cells within the cell cycle was determined microscopically after staining the nuclei with Hoechst 33258.

Protein electrophoresis and immunoblotting

Proteins were extracted according to Freudenreich & Nick (1998). The cells were harvested by filtration on nylon mesh as above, and 1 g of biomass was homogenized immediately in liquid nitrogen with a pestle and mortar. The frozen powder was mixed 3 : 1 (w/v) with extraction buffer [25 mM MES (2-morpholinoethanesulfonic acid), 5 mM EGTA, 5 mM $MgCl_2$, 1 M glycerol, 1 mM guanosine 5′-triphosphate (GTP), 1 mM dithiothreitol, 1 mM phenyl methyl sulphonyl fluoride, 1 μM aprotinin, 1 μM leupeptin, 1 μM pepstatin, pH 6.9]. The mixture was allowed to thaw on ice. A 50-μL aliquot of the resulting extract was used as a total protein fraction. The thawed mixture was centrifuged at 3000 *g* for 15 min at 4 °C, and the supernatant centrifuged again at 18 000 *g* for 1 h at 4 °C. The final supernatant was used as the soluble fraction and the pellet represented the sedimentable fraction. The fractions were mixed with denaturing buffer [50 mM Tris-HCl, pH 6.9; 2% (w/v) sodium dodecyl sulphate (SDS); 36% (w/v) urea; 30% (w/v) glycerol; 5% (v/v) β-mercaptoethanol; 0.5% (w/v) bromophenol blue]. Protein concentration was determined after staining with amidoblack (Popov, Schmitt & Mathies 1975). Samples were vortexed, boiled for 5 min and separated by SDS-polyacrylamide gel electrphoresis (PAGE) on 10% (w/v) acrylamide gels. Separated proteins were either visualized by staining with Coomassie Brilliant Blue or transferred onto polyvinylidene difluoride (PVDF) membranes by semi-dry electro-blotting for probing with antibodies. Mouse monoclonal antiα-tubulin N356 (Amersham Biosciences) and mouse monoclonal antiactin 69100, clone C4 (ICN Biochemicals Inc., Irvine, CA, USA) antibodies were used at 1 : 4000 dilution. After incubation with

antimouse horseradish peroxidase-conjugated secondary antibody (ICN), proteins were visualized by means of a chemiluminiscence ECL detection kit (Amersham) on X-ray films (Foma, Hradec Králové, Czech Republic).

RESULTS

Organization of cytoplasm and cell viability during treatment at 0 °C and after recovery at 25 °C

When cultivated at the control temperature of 25 °C, interphase cells formed many radially oriented cytoplasmic strands that connected the cortical and perinuclear regions (Fig. 1a). Cold treatment in ice water (0 °C) led to gradual disruption of the cytoplasmic strands, starting in all cells after only 5 min of cold treatment (data not shown). The cytoplasmic strands then gradually disappeared, the vacuolar complex fused into one big central vacuole, and the nucleus shifted into the layer of cortical cytoplasm. After 12 h at 0 °C, virtually no cytoplasmic strands were observed (Fig. 1b). Restoration of cytoplasmic strands in the surviving cells started within 5 min after transfer to 25 °C (Fig. 1c), and numerous cytoplasmic strands reappeared after 20 min (Fig. 1d).

The viability of cells maintained at 0 °C was assessed periodically (after each additional 2 h of recovery at 25 °C) using FDA staining (Widholm 1972). Figure 1e shows the decline in cell viability during the 12 h at 0 °C in a representative experiment. At the end of the 12 h at 0 °C, the cell

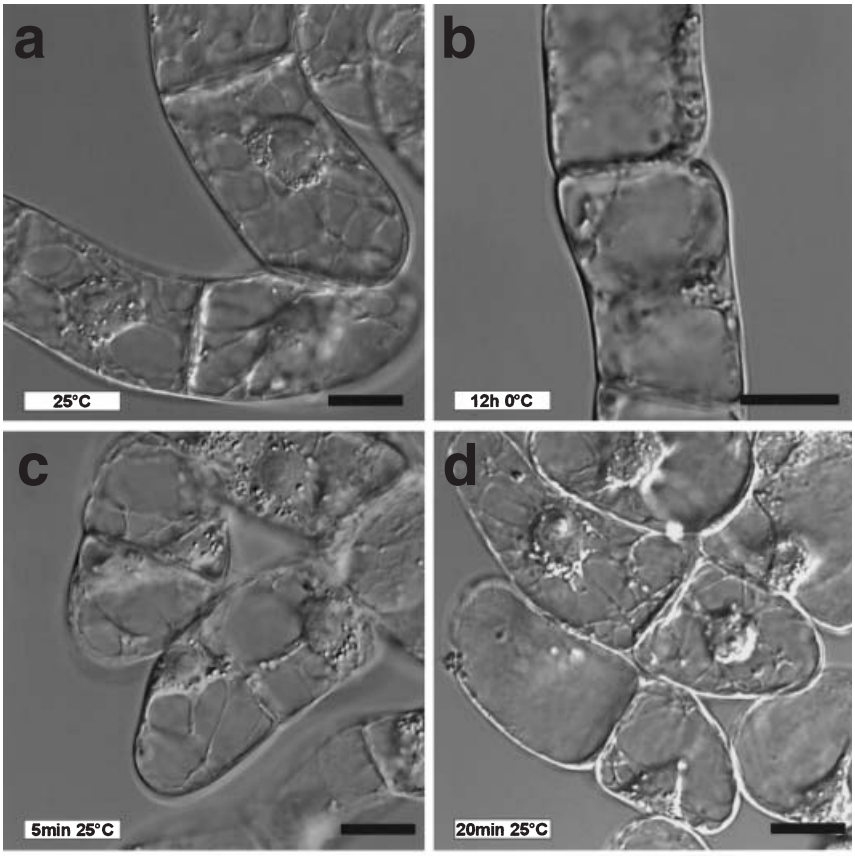

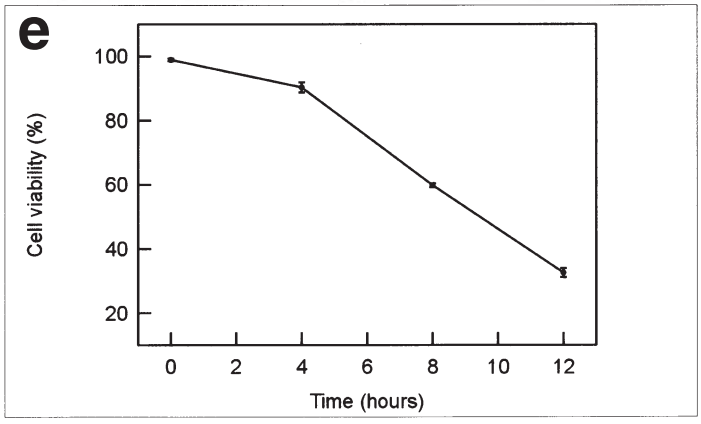

Figure 1. Changes in the spatial organization of the cytoplasm (Nomarski DIC) and cell viability in 3-day-old tobacco BY-2 cells exposed to 0 °C and during subsequent incubation at 25 °C. (a) Control cells with transvacuolar cytoplasmic strands connecting the cytoplasm around the nucleus with the cortical cytoplasm. (b) Breakdown of transvacuolar cytoplasmic strands in cells maintained at 0 °C for 12 h. (c) Re-formation of transvacuolar cytoplasmic strands in cells after 5 min recovery at 25 °C following 12 h at 0 °C. (d) Reconstitution of cytoplasmic strands after 20 min at 25 °C. Bars = 20 μm (e) Viability of 3-day-old BY-2 cells maintained at 0 °C for 0–12 h. The graph shows a representative trend in the decrease in viability during the cold treatment (FDA test performed after 2 h recovery at 25 °C for each time point). Error bars represent SE (n = 5 slides, 400 cells were assessed on each slide).

viability varied between 30 and 50% in four independent experiments.

De-polymerization of actin filaments and microtubules in cells exposed to 0 °C

In tobacco BY-2 cells maintained at 25 °C, AFs were detectable in three cytoplasmic regions: in the cortical layer of cytoplasm (Fig. 2a), in the perinuclear region, and in the transvacuolar cytoplasmic strands (Fig. 2b). AFs in the cortical layer of cytoplasm formed a dense network of thick filaments traversing the cortical cytoplasm in all directions. In addition, fine, parallel filaments oriented transversely to the long cell axis were often detectable (Fig. 2a). AFs in the perinuclear region formed a basket-like structure around the nucleus (Fig. 2b). Cytoplasmic strands connecting the

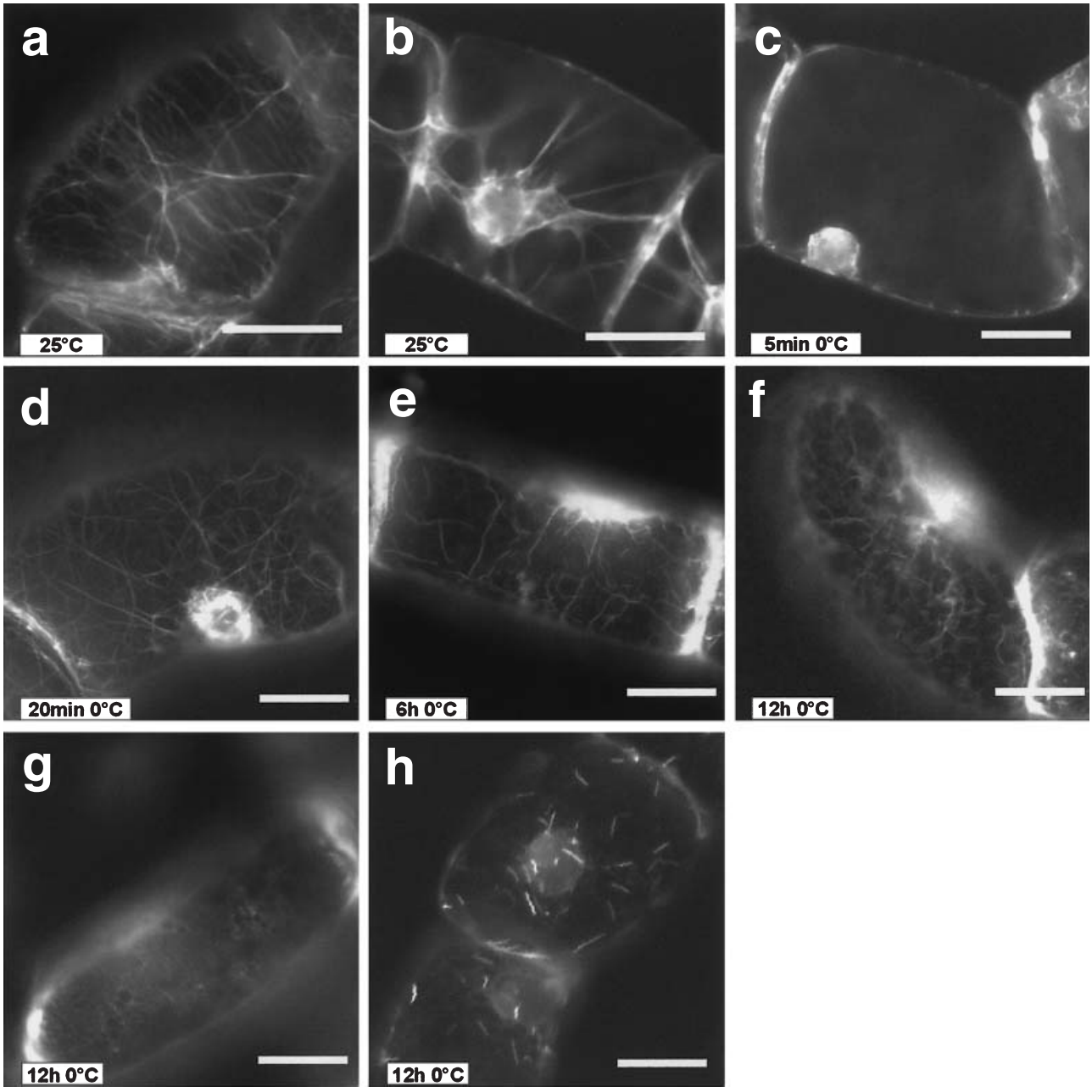

Figure 2. AFs in 3-day-old BY-2 cells maintained at 0 °C for 0–12 h. Rhodamin-phalloidin staining. (a) A complex actin network in the cortical cytoplasm of control cells. Optical section of the cortical cytoplasm. (b) Actin filaments in transvacuolar strands and around nucleus in control cells. Median optical section. (c) Loss of radial AFs in transvacuolar strands after 5 min at 0 °C. Median optical section. (d) Absence of transverse AFs and formation of a cortical network of thick, disoriented AFs in cells incubated at 0 °C for 20 min. (e) Advanced disassembly of AFs in the cortical cytoplasm of cells exposed to 0 °C for 6 h. (f, g, h) A few thick AFs remaining in the cortical cytoplasm (f), completely disassembled AFs (g), and actin rods (h) in cells exposed to 0 °C for 12 h. Bars = 20 μm.

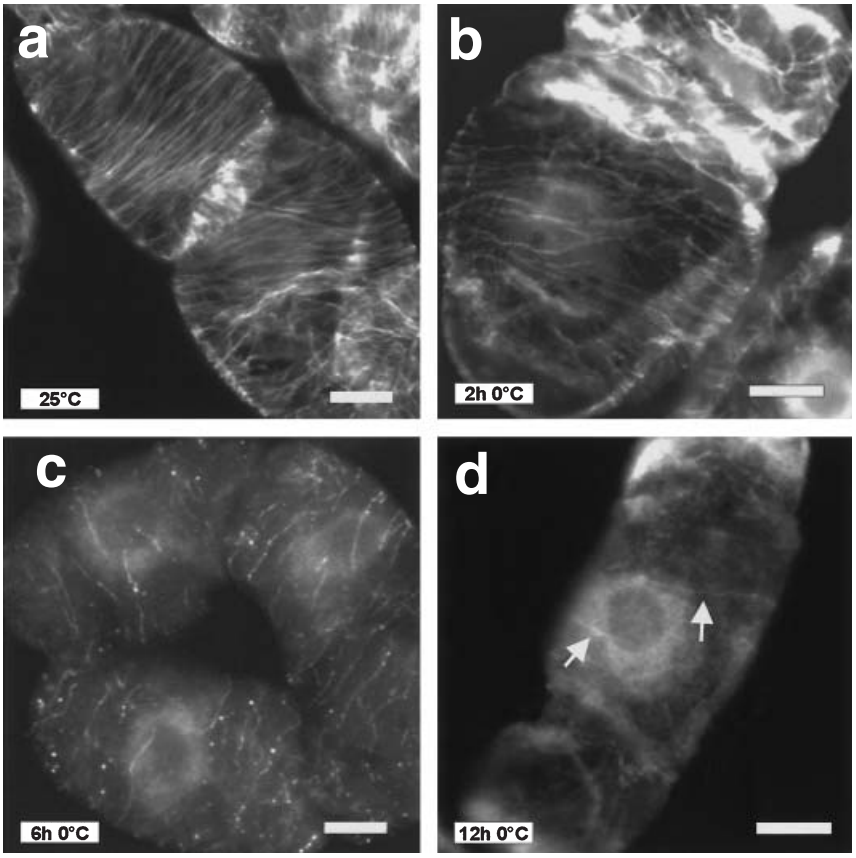

Figure 3. MTs in 3-day-old BY-2 cells maintained at 0 °C for 0–12 h. Immunofluorescence staining with antiα-tubulin antibody and FITC-conjugated secondary antibody. (a) Cortical transverse MT arrays in control cells. (b, c) Gradual de-polymerization of cortical MTs after 2 h (b) and 6 h (c) of exposure to 0 °C. (d) De-polymerized MTs in cells exposed to 0 °C for 12 h. Note the few short MTs (arrows) persisting in the cortical region. Bars = 10 μm.

perinuclear and cortical regions were filled with thick AFs, forming a radial AF array (Fig. 2b).

The first observable effects of the cold treatment, which became apparent after 5 min at 0 °C, were the degradation of the cytoplasmic strands and disappearance of the radial AF array (Fig. 2c). After 20 min, the transversely oriented, fine, parallel AFs in the cortex disappeared and actin re-formed into a network of disordered, thick and branched AFs (Fig. 2d). This network gradually thinned out during the first 6 h of cold treatment, leaving only a sparse actin network in the cortical region in successfully stained cells (Fig. 2e). Very rarely (in about 1% of cells), brightly shining actin rods or dots appeared in the cortex and around the nucleus. Such actin rods or dots were never detected in the controls. After 12 h of cold treatment, only 19% of the cells retained any AFs, and these were few in number, short, and sometimes branched AFs (Fig. 2f). However, the number of cells with actin rods or dots in the cortex and around the nucleus (Fig. 2h) increased to 18%. A total of 24% of the cells did not contain any detectable actin filaments (Fig. 2g), and 39% of the cells were damaged. The relative incidence of individual AF categories in controls and cells exposed to 0 °C for 12 h is illustrated in Fig. 4a and c.

As expected, MTs in interphase cells at control temperature formed parallel cortical arrays, oriented transversely or at an oblique angle to the long axis of the cell (Fig. 3a). In contrast to AFs, no MTs were seen in the cytoplasmic strands or around the nucleus. Disassembly of MTs commenced within 20 min of cold treatment (data not shown). After 2–6 h, cortical MTs gradually de-polymerized (Fig. 3b & c). After 12 h, only 8% of the cells contained short MT fragments in transverse orientation (Fig. 3d, arrows), whereas 42% of the cells did not contain any polymerized tubulin and 50% of the cells were damaged. The relative incidence of individual MT structures in controls and in cells exposed to 0 °C for 12 h is illustrated in Fig. 4b and d.

Re-polymerization of AFs and MTs during recovery at control temperature

After only 30 s at 25 °C, various forms of polymerized actin were detectable in the cortical cytoplasm as well as around the nucleus in all successfully stained cells (54%). The actin forms were: (a) actin dots (Fig. 5a); (b) actin rods often connected with thin AFs (Fig. 5b); (c) actin dots connected with thin branched AFs resembling 'beads-on-string' with brightly shining dots often localized to the junction of Y-shaped filament (Fig. 5c & d); and (d) a very dense network of thin filaments (Fig. 5e). These structures appeared only transiently during the early phases of the recovery period. After 15 min at 25 °C, around 45% of cells re-formed a sparse network of thicker AFs (Fig. 5f) although the transient actin structures were still detectable in about 10% of the cells. After 30 min at 25 °C, all successfully stained cells (approximately 60%) re-formed a sparse network of thick

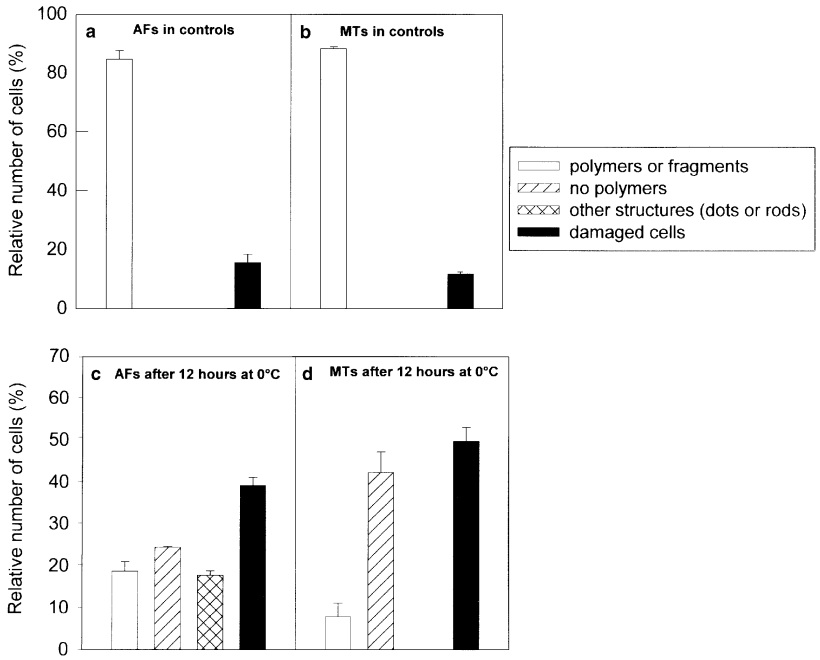

Figure 4. Frequencies of individual categories of AFs and MTs staining in control cells and in cells after 12 h at 0 °C. (a, b) Frequencies of staining categories of AFs (a) and MTs (b) in control cells. (c, d) Frequencies of staining categories of AFs (c) and MTs (d) in cells maintained at 0 °C for 12 h. Individual categories used for quantification are: cytoskeletal polymers or their fragments (white columns), totally de-polymerized cytoskeleton (shaded columns), other structures as dots and rods (checkered columns), and damaged cells (black columns). Error bars represent SE (n = 5, 6, 3 and 9 slides, for a, b, c and d, respectively; 300 cells assessed on each).

AFs in the cortical region. After 1 h at 25 °C, no transient actin structures were detectable and stained cells contained control-like AFs network in the cortical cytoplasm (Fig. 5g). Simultaneously with the re-formation of the cortical actin network, reorganization of the actin cytoskeleton also occurred around the nucleus during the recovery period. Initially, the diffuse signal from de-polymerized AFs that was detectable during the cold treatment re-formed into filaments sometimes decorated with dots. After 5 min at 25 °C, AFs formed a dense basket surrounding the nucleus (Fig. 5h, arrows). At the same time, other AFs emerged from the basket, pointing towards the cortical region (Fig. 5h, arrowheads). After 15 min recovery, AFs also re-formed in the fully developed transvacuolar cytoplasmic strands (Fig. 5i & j).

Newly polymerized short and randomly oriented MTs were detected in the cortical cytoplasm of interphase cells after 1 min of recovery at 25 °C (Fig. 6a). After 5 min, the randomly oriented MTs elongated and formed a dense network (Fig. 6b). Within 1 h, the cortical MTs formed parallel, transverse arrays as in the controls (Fig. 6c). In cells at preprophase and early G1, polymerization of MTs was also seen at the nuclear surface (Fig. 6d & e). Polymerization of MTs around the nucleus was transient, however, occurring only during the first few minutes of recovery, simultaneously with the polymerization of MTs in the cortex. After 1 h of recovery, only control-like MT arrays were detected in the cortical cytoplasm of the cells.

Western blot analysis of cytoskeletal proteins during cold treatment

To test for possible changes in association of cytoskeletal proteins with membranes during the cold treatment, the total, soluble and sedimentable protein fractions were analysed by SDS-PAGE and immunoblotting of actin and tubulin. Equal amounts of proteins from all fractions taken at 2-h intervals during the 12 h at 0 °C were loaded onto gels for the analysis. The immunoblots show that the relative amounts of actin (Fig. 7a) and α-tubulin (Fig. 7b) in the total, soluble, and sedimentable protein fractions did not change substantially during the whole cold treatment.

DISCUSSION

Cold-stressed tobacco BY-2 cells proved to be a highly sensitive experimental model for detailed investigation of the processes of de-polymerization and re-assembly of the actin and microtubular cytoskeleton. Exposing the cells to 0 °C for only a few minutes affected both their cytoplasmic architecture and particularly the organization of the cytoskeleton. Although the cold treatment affected the viability of many cells, almost half of the cells were able to recover after transfer to normal temperature, thereby facilitating studies of the sites of AF and MT initiation and polymerization.

The results obtained by the FDA viability tests are based on detection of active processes in living cells, namely, enzymatic activities and membrane integrity (Steward *et al.* 1999). Since cells just released from 0 °C generally have very low enzymatic activities as well as cold-damaged membranes (Kacperska 1999), an immediate use of the FDA test would be unsuitable. Therefore, the viability of cells released from the cold treatment was assessed after an additional 2 h of recovery at 25 °C. Using this approach, the cell viability varied between 50 and 30% at the end of 12 h at 0 °C in four independent experiments. These data are consistent with the number of cells with

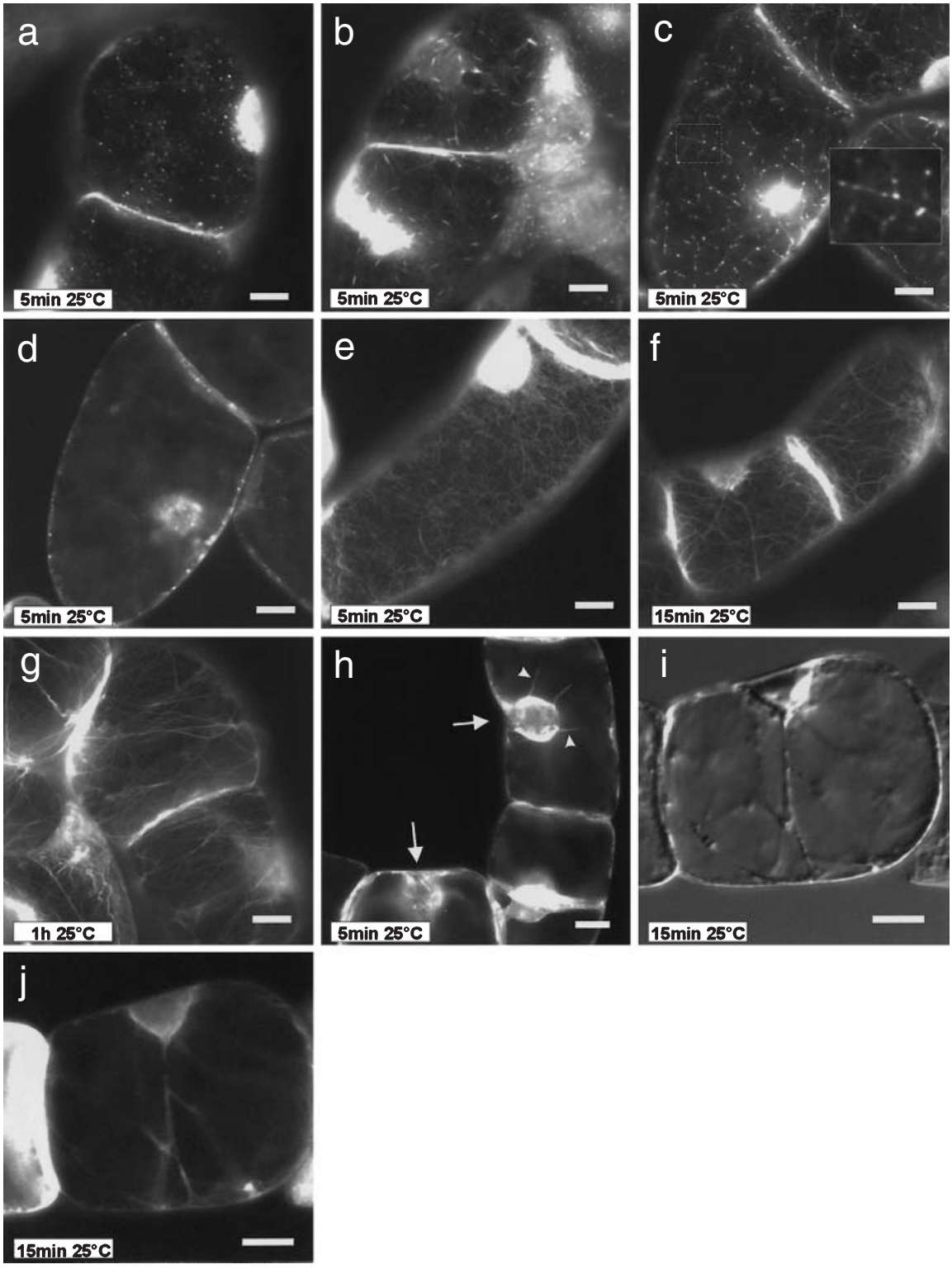

Figure 5. Recovery of tobacco BY-2 AFs after 12 h at 0 °C and subsequent incubation at 25 °C. Rhodamin-phalloidin staining (a–g, i, j) Nomarski DIC (H). (a–e) Transient actin structures formed in the cortical region and around nucleus during 5 min recovery at 25 °C. (a) Actin dots; (b) short actin rods connected with thin filaments; (c) disoriented branched thin filaments with a dotted signal in the cortical cytoplasm (inset shows magnification of Y-shaped actin filaments with dotted signal); (d) actin around the nucleus; (e) dense cortical network that consisted of very thin AFs. (f) Cortical actin network after 15 min at 25 °C. (g) Cortical actin network after 1 h at 25 °C. (h) Basket-like actin structure formed around the nucleus (arrows) after 5 min at 25 °C. AFs emerging from the basket towards the cortical region are indicated with arrowheads. (i, j) Formation of AFs in transvacuolar strands. (i) First transvacuolar cytoplasmic structures formed during 15 min at 25 °C. (j) AFs in transvacuolar strands in the same cell. Bars = 10 μm.

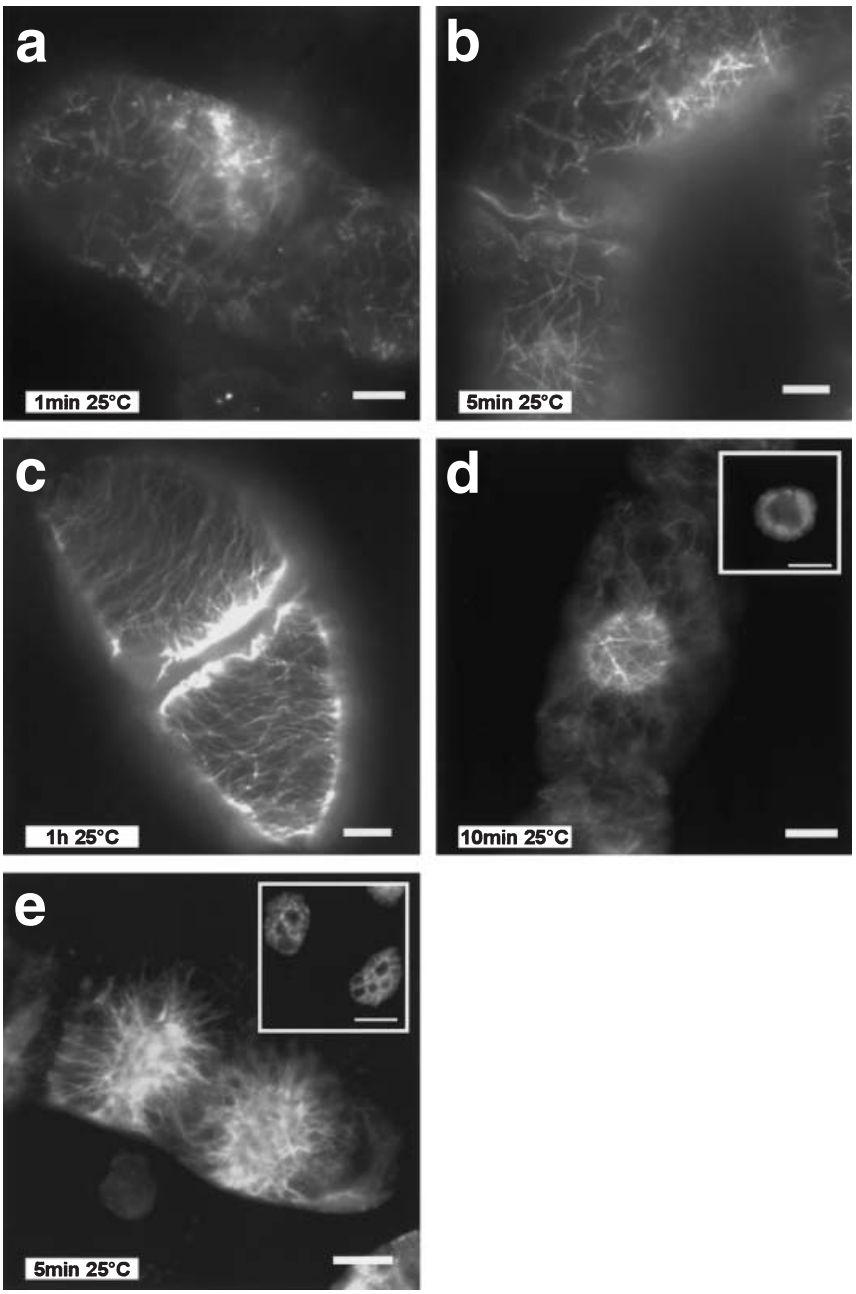

Figure 6. Recovery of tobacco BY-2 MTs after 12 h at 0 °C and subsequent incubation at 25 °C. (a–e) Immunofluorescence staining with antiα-tubulin antibody and FITC-conjugated secondary antibody. (Inserts in d, e) DNA staining with Hoechst 33258. (a, b) Polymerization of MTs in the cortical cytoplasm after 1 min (a) and 5 min (b) at 25 °C. Newly polymerized MTs were disorganized. (c) Cortical MTs after 1 h at 25 °C. (d) Polymerization of MTs around the preprophase nucleus (see inset) after 10 min at 25 °C. (e) Polymerization of tubulin on the surface of early G1 nuclei after 2 min at 25 °C. Newly polymerized MTs emerged from nuclear surface of early G1 nuclei (see inset) towards the cortical region. Bars = 10 μm.

unsuccessfully stained cytoskeleton. The percentage of such cells was 10–15% in the controls but increased to approximately 40% for AFs and 50% for MTs after 12 h at 0 °C, suggesting that most of these cells may have died during the cold treatment.

We have found that AFs in the transvacuolar cytoplasmic strands disappeared within 5 min at 0 °C, simultaneously with the disintegration of the cytoplasmic strands as seen with the Nomarski DIC. Woods, Reid & Patterson (1984) have observed similar disintegration of cytoplasmic strands in response to cold in various plant species, and suggested that this was the result of disruption of AFs. Indeed, the scaffolding role of AFs in the formation of transvacuolar strands has been demonstrated in experiments using actin de-polymerizing drugs. A breakdown of cytoplasmic strands was observed after treating tobacco BY-2 cells with latrunculin B for 60 min (Van Gestel *et al.* 2002) or root hairs of *Vicia sativa* with cytochalasin D for 30 min (Esseling *et al.* 2000). Therefore the disruption of the transvacuolar cytoplasmic strands observed in our experiments is likely to be the result of cold-induced de-polymerization of the constituent AFs. The transverse AFs in the cell cortex were apparently less sensitive to cold, de-polymerizing within 20 min of the cold treatment, at the same time as the first signs of degradation of the cortical MTs. Possibly the destabilization of one resulted in disorganization of the other, in a manner similar to that shown by Blancaflor (2000) by selective drug-induced stabilization or destabili-

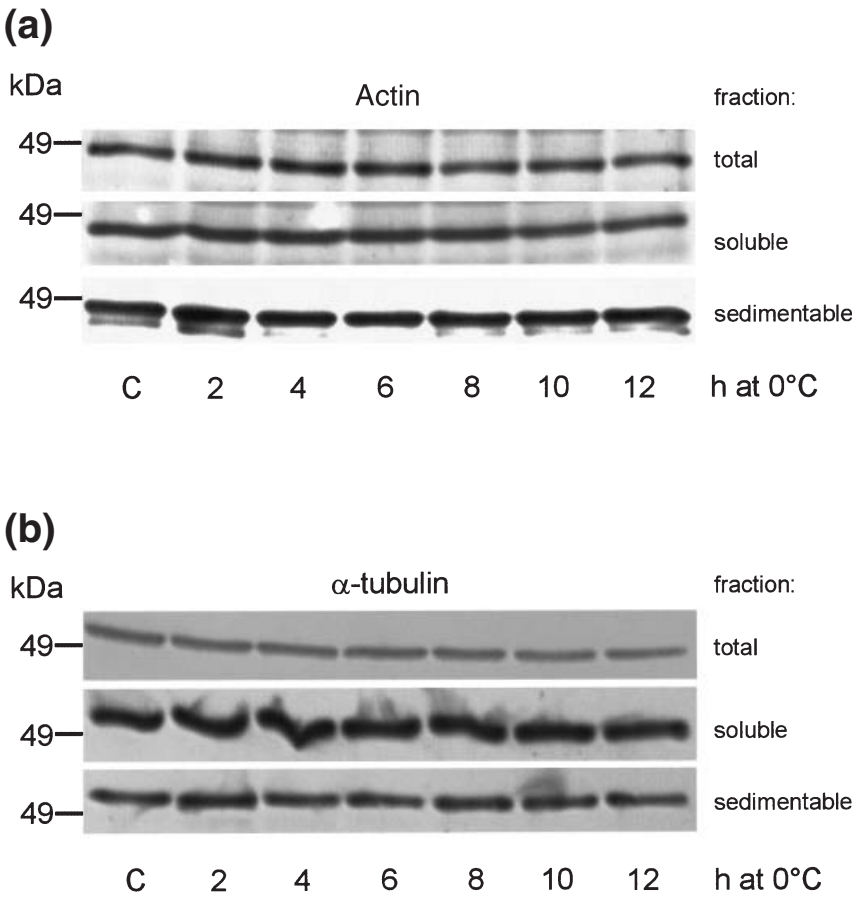

Figure 7. Western blot analysis of cytoskeletal proteins in the total, soluble, and sedimentable protein extracts from BY-2 cells incubated 0–12 h at 0 °C. Immunoblots were probed with antiactin (a) and antiα-tubulin (b) antibodies.

zation of the actin and microtubular cytoskeleton, suggesting co-operation of actin and microtubules in the cortical cytoplasm. In our experiments, the most resistant actin structures were the thick actin cables that endured in the cortical cytoplasm even after prolonged cold treatment. This is in agreement with the results of Egierszdorff & Kacperska (2001), who demonstrated that thick actin cables in oilseed rape cell suspension were generally more resistant to freezing temperature than the fine filamentous network. Actin rods, which were observed at the end of the cold period in some cells, may represent a population of highly stable, short actin filaments. However, further investigation will be necessary to elucidate the composition of these actin structures and to determine whether they originate by severing of existing filaments or by *de novo* polymerization at 0 °C.

Our study of AFs included a comparison with MTs. Although data concerning the cold-stability or sensitivity of MTs in tobacco BY-2 cells are available in the literature, they are surprisingly inconsistent. For example, high cold-resistance of tobacco BY-2 MTs has been reported by Hasezawa *et al*. (1997) who showed that the MTs were not completely destroyed by treatment at 0 °C for 3 h. In contrast, Mizuno (1992) showed that all cortical MTs in exponentially growing tobacco BY-2 cells (2-day-old) were highly cold-sensitive; treatment for 30 min at 0 °C resulted in their complete disappearance. In our results, approximately 8% of cells still contained a few short fragments of tubulin polymers even at the end of 12 h at 0 °C, indicating that they are highly cold stable. We did not observe any newly formed, cold-induced microtubular structures similar to those seen in *Chaetomorpha moniligera* (Mizuta, Kaneko & Tsurumi 1995).

The immunoblot analysis did not detect any appreciable changes in the amounts of soluble and sedimentable actin or tubulin during the whole cold treatment, indicating that cytoskeletal monomers did not undergo any substantial subcellular redistribution after the disintegration of the polymers. We also have found that translational activity was severely reduced by the cold treatment (unpublished results). Therefore it seems that the pool of cytoskeletal proteins was stable, did not degrade, and was not augmented by newly synthesized proteins.

Incubation of cells at 0 °C for 12 h was apparently sufficient to de-polymerize most AFs and MTs. After transfer back to 25 °C, a rapid re-polymerization of actin into small dots and rods occurred within 30 s of recovery. As these structures appeared both in the cortical region and around the nucleus, independent nucleation sites are presumably located in these two regions. The formation of the unique transient actin structures during the early stages of actin re-polymerization is of particular interest. To our knowledge,

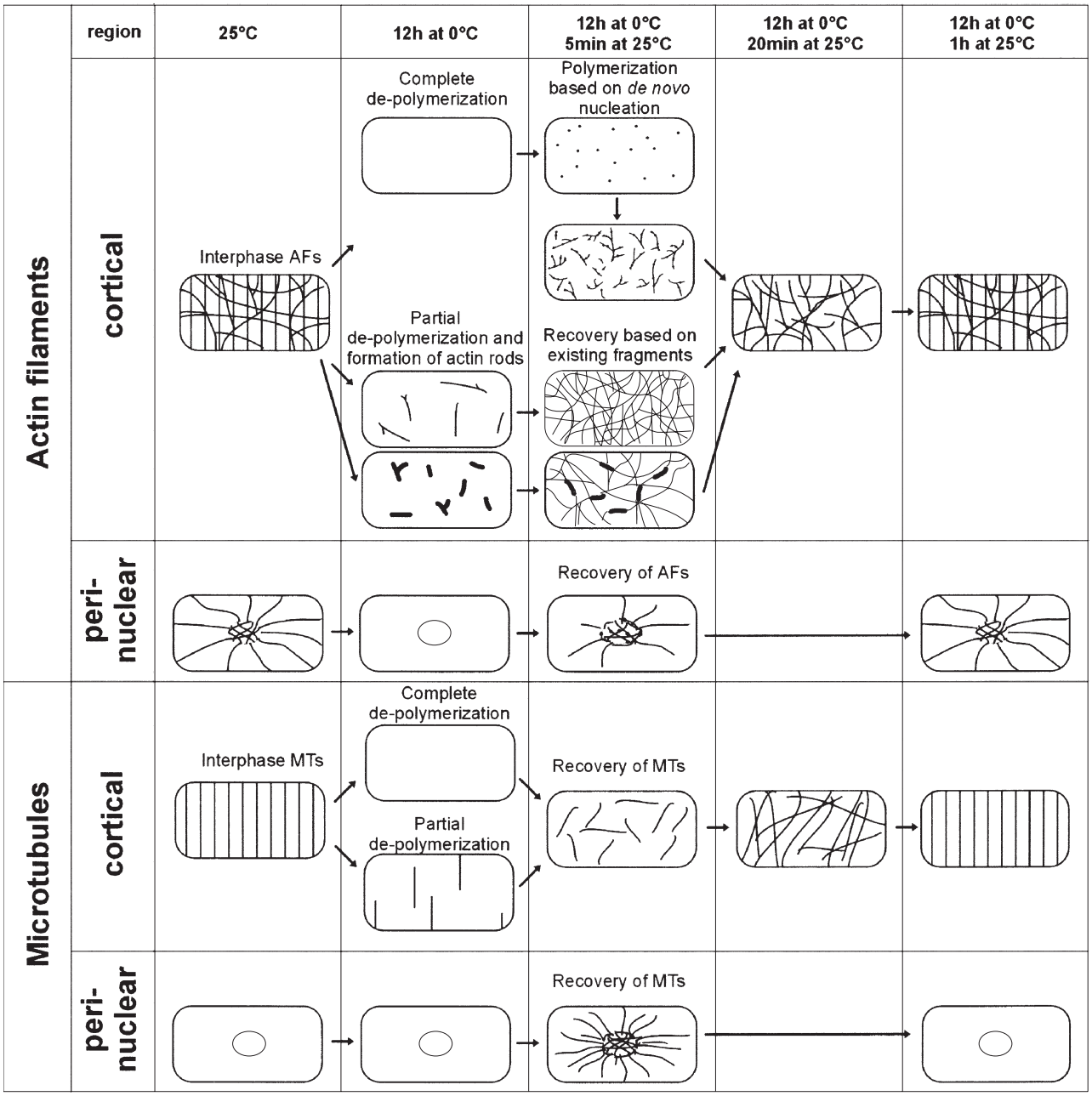

Figure 8. A model summarizing important stages in the reorganization of cytoskeleton during cold treatment at 0 °C and subsequent recovery at 25 °C in interphase BY-2 cells. Arrows indicate proposed course of cytoskeletal reorganization. Cold treatment resulted in complete de-polymerization of AFs in the perinuclear region and in the cytoplasmic strands, and complete or partial de-polymerization in the cortical region. Polymerization of actin into dots in the cell cortex and in the perinuclear region during early phases of recovery probably occurred in those cells in which cold-induced de-polymerization was complete. The cells retaining short fragments of actin at the end of the cold treatment were able to polymerize actin into net immediately, without formation of actin dots. In the perinuclear region, an actin basket was formed around the nucleus during early phases of recovery. AFs emerged from it pointing towards the cortical region, re-forming actin in the cytoplasmic strands. In some cells, transient actin structures were also formed in the perinuclear region during early phases of recovery. As with AFs, cold also induced complete or partial de-polymerization of MTs. During early phases of recovery, the elongating MTs in the cortical region were always disoriented. Their transversal orientation was established later during recovery. Excepting during the G2 phase of the cell cycle, MTs were not detected in the perinuclear region in interphase control cells. However, re-polymerization of microtubules initiated at the nuclear envelope was detected in some cells during early phases of recovery.

the incidence of similar transient actin structures in plant cells has not been described. We propose that the formation of actin dots and rods in the cortex and around the nucleus represent sites of actin nucleation and polymerization. The appearance of the thin and branched actin filaments connecting the dots and rods ('beads-on-string' structures, or bright dots at the junctions of Y-shaped filaments) later during the recovery period is presumably the outcome of AF assembly from the initiation sites. The structure and function of actin nucleation centres are only beginning to be understood in plants (reviewed in Vantard & Blanchoin 2002). It seems likely that the Arp2/3 protein complex, which plays a key role in *de novo* AF polymerization in protozoa, fungi, and animals (Machesky & Gould 1999), is also involved in AF nucleation in plants, since mutations Arp2 and Arp3 genes affect actin organization and cell shape in *Arabidopsis thaliana* (Mathur *et al*. 2003). Moreover, the transient, branched AFs shown here resemble those induced by the Arp2/3 complex (Svitkina & Borisy 1999). It remains to be established whether the transient dots and rods in our experiments do indeed co-localize with components of the Arp2/3 complex.

Some cells formed a dense actin network without any dotted signal within 30 s after transfer to control temperature. Different modes of actin re-polymerization were probably connected with the severity of the preceding cold-induced AFs de-polymerization. In cells in which actin de-polymerization was complete, re-assembly required *de novo* nucleation of new actin filament by actin-nucleation sites. In cells that retained some remnants of AFs, re-assembly could presumably occur by means of addition of new monomers to existing free filament ends. In the latter case, no transient actin structures would be formed and an actin network would be detectable immediately.

Similarly to that of AFs, the polymerization of MTs was a very rapid process. Within 1 min after transfer to control temperature, disoriented MTs appeared in the cortical cytoplasm, although their transverse position was not established until later. Randomly oriented newly polymerized MTs after cold-induced de-polymerization, as well as their subsequent rearrangement into transverse orientation during warming, have also been reported for *Closterium ehrenbergii* (Hogetsu 1986). The author suggested that MT nucleation and ordering are governed by two independent mechanisms. Our data support this hypothesis. We showed that, simultaneously with the polymerization of cortical MTs, another set of MTs elongated from the perinuclear region towards the cortical cytoplasm within 1 min of recovery. The most massive polymerization on the nuclear surface was observed in cells at late telophase/early G1 phase. This observation is consistent with previous reports that the nuclear envelope plays an important role in the polymerization of MTs (Stoppin *et al*. 1994), especially in this phase of the cell cycle (Nagata & Hasezawa 1993).

An overview of our observations of changes in the organization of AFs and MTs during cold treatment and subsequent recovery is depicted in Fig. 8, together with a proposed course of reorganization of the actin and microtubular cytoskeleton.

ACKNOWLEDGMENTS

This work was supported by grants from the ministry of Education, Youth, and Sports of the Czech Republic, No. VZ113100003, and from the Grant Agency of the Academy of Sciences of the Czech Republic, No. A5038207. The authors thank Vlasta Sakařová and Halka Hrabáková for their technical assistance.

REFERENCES

Akashi T., Kawasaki S. & Shibaoka H. (1990) Stabilization of cortical microtubules by the cell wall in cultured tobacco cells. *Planta* **182,** 363–369.

Blancaflor E.B. (2000) Cortical actin filaments potentially interact with cortical microtubules in regulating polarity of cell expansion in primary roots of maize (Zea mays L.). *Journal of Plant Growth Regulation* **19,** 406–414.

Condeelis J. (2001) How is actin polymerization nucleated in vivo? *Trends in Cell Biology* **11,** 288–293.

Egierszdorff S. & Kacperska A. (2001) Low temperature effects on growth and actin cytoskeleton organisation in suspension cells of winter oilseed rape. *Plant Cell Tissue and Organ Culture* **65,** 149–158.

Erhardt M., Stoppin-Mellet V., Campagne S., *et al.* (2002) The plant Spc98p homologue colocalizes with gamma-tubulin at microtubule nucleation sites and is required for microtubule nucleation. *Journal of Cell Science* **115,** 2423–2431.

Esseling J., de Ruijter N. & Emons A. (2000) The root hair actin cytoskeleton as backbone, highway, morphogenetic instrument and target for signalling. In *Root Hairs. Cell and Molecular Biology* (eds R.W. Ridge & A.M.C. Emons), pp. 29–52. Springer-Verlag, Tokyo, Japan.

Freudenreich A. & Nick P. (1998) Microtubular organization in tobacco cells: Heat-shock protein 90 can bind to tubulin *in vitro*. *Botanica Acta* **111,** 273–279.

Hasezawa S., Kumagai F. & Nagata T. (1997) Sites of microtubule reorganization in tobacco BY-2 cells during cell-cycle progression. *Protoplasma* **198,** 202–209.

Hogetsu T. (1986) Re-formation of microtubules in *Closterium ehrenbergii meneghini* after cold-induced depolymerization. *Planta* **167,** 437–443.

Kacperska A. (1999) Plant responses to low temperature: signalling pathways involved in plant acclimation. In *Cold-Adapted Organisms* (eds R. Margesin & F. Schinner), pp. 79–104. Springer-Verlag Berlin Heidelberg, Germany.

Kakimoto T. & Shibaoka H. (1987) Actin filaments and microtubules in the preprophase band and phragmoplast of tobacco cells. *Protoplasma* **140,** 181–186.

Knop M. & Schiebel E. (1997) Spc98p and Spc97p of the yeast gamma-tubulin complex mediate binding to the spindle pole body via their interaction with Spc110p. *EMBO Journal* **16,** 6985–6995.

Liebe S. & Menzel D. (1995) Actomyosin-based motility of endoplasmic reticulum and chloroplasts in Vallisneria mesophyll cells. *Biology of the Cell* **85,** 207–222.

Machesky L.M. & Gould K.L. (1999) The Arp2/3 complex: a multifunctional actin organizer. *Current Opinion in Cell Biology* **11,** 117–121.

Mathur J., Mathur N., Kernebeck B. & Hulskamp M. (2003) Mutations in actin-related proteins 2 and 3 affect cell shape development in Arabidopsis. *Plant Cell* **15,** 1632–1645.

Mizuno K. (1992) Induction of cold stability of microtubules in cultured tobacco cells. *Plant Physiology* **100,** 740–748.

Mizuta S., Kaneko M. & Tsurumi S. (1995) Assembly of cortical microtubules during cold treatment of the coenocytic green alga, *Chaetomorpha moniligera*. *Planta* **196,** 190–192.

Murphy S.M., Urbani L. & Stearns T. (1998) The mammalian gamma-tubulin complex contains homologues of the yeast spindle pole body components Spc97p and Spc98p. *Journal of Cell Biology* **141,** 663–674.

Nagata T. & Hasezawa S. (1993) Events at the border between the M and G_1 phases in highly synchronized culture of tobacco BY-2 cells. *Journal of Plant Research* **3,** 29–35.

Nagata T., Nemoto Y. & Hasezawa S. (1992) Tobacco BY-2 cell line as the 'HeLa' cell in the cell biology of higher plants. *International Review of Cytology* **132,** 1–30.

Nebenführ A., Gallagher L.A., Dunahay T.G., Frohlick J.A., Mazurkiewicz A.M., Meehl J.B. & Staehelin L.A. (1999) Stop-and-go movements of plant Golgi stacks are mediated by the acto-myosin system. *Plant Physiology* **121,** 1127–1141.

Nick P. (2000) Control of the response to low temperatures. In: *Plant Microtubules Potential for Biotechnology* (ed. P. Nick), pp. 121–135. Springer-Verlag. Berlin, Heidelberg, Germany.

Olyslaegers G. & Verbelen J.P. (1998) Improved staining of F-actin and co-localization of mitochondria in plant cells. *Journal of Microscopy – Oxford* **192,** 73–77.

Örvar B.L., Sangwan V., Omann F. & Dhindsa R.S. (2000) Early steps in cold sensing by plant cells: the role of actin cytoskeleton and membrane fluidity. *Plant Journal* **23,** 785–794.

Popov N., Schmitt S. & Mathies H. (1975) Eine störungsfreie Mikromethode zur Bestimmung des Proteingehaltes in Gewebshomogenaten. *Acta Biologica Germanica* **34,** 144–146.

Quader H., Hofmann A. & Schnepf E. (1989) Reorganization of the endoplasmic reticulum in epidermal cells of onion bulb scales after cold stress: involvement of cytoskeletal elements. *Planta* **177,** 273–280.

Steward N., Martin R., Engasser J.M. & Goergen J.L. (1999) A new methodology for plant cell viability assessment using intracellular esterase activity. *Plant Cell Reports* **19,** 171–176.

Stoppin V., Vantard M., Schmit A.C. & Lambert A.M. (1994) Isolated plant nuclei nucleate microtubule assembly: the nuclear surface in higher plants has centrosome-like activity. *Plant Cell* **6,** 1099–1106.

Svitkina T.M. & Borisy G.G. (1999) Arp2/3 complex and actin depolymerizing factor cofilin in dendritic organization and treadmilling of actin filament array in lamellipodia. *Journal of Cell Biology* **145,** 1009–1026.

Takagi S. (2000) Roles for actin filaments in chloroplast motility and anchoring. In *Actin, a Dynamic Framework for Multiple Plant Cell Function* (eds C.J. Staiger, F. Baluska, D. Volkmann & P.W. Barlow), pp. 203–212. Kluwer Academic Publishers, Dordrecht, The Netherlands.

Van Gestel K., Kohler R.H. & Verbelen J.P. (2002) Plant mitochondria move on F-actin, but their positioning in the cortical cytoplasm depends on both F-actin and microtubules. *Journal of Experimental Botany* **53,** 659–667.

Vantard M. & Blanchoin L. (2002) Actin polymerization processes in plant cells. *Current Opinion in Plant Biology* **5,** 502–506.

Wick S., Seagull R., Osborn M., Weber K. & Gunning B. (1981) Immunofluorescence microscopy of organized microtubule arrays in structurally stabilized meristematic plant cells. *Journal of Cell Biology* **89,** 685–690.

Widholm J.M. (1972) The use of fluorescein diacetate and phenosafranine for determining viability of cultured plant cells. *Stain Technology* **47,** 189–194.

Wiese C. & Zheng Y.X. (1999) Gamma-tubulin complexes and their interaction with microtubule- organizing centers. *Current Opinion in Structural Biology* **9,** 250–259.

Woods C.M., Reid M.S. & Patterson B.D. (1984) Response to chilling stress in plant cells. 1. Changes in cyclosis and cytoplasmic structure. *Protoplasma* **121,** 8–16.

Received 7 March 2003; received in revised form 14 October 2003; accepted for publication 26 November 2003